Optik 127 (2016) 3143–3149

Contents lists available at ScienceDirect

Optik

journal homepage: www.elsevier.de/ijleo

Performance of eliminating sun glints reflected off wave surface by polarization filtering under influence of waves

Guocong Wang[a,b], Jianli Wang[a,*], Zhenduo Zhang[a], Bochuan Cui[a,b]

[a] Changchun Institute of Optics, Fine Mechanics and Physics, Chinese Academy of Sciences, Changchun 130033, Jilin, China
[b] University of Chinese Academy of Sciences, Beijing 100049, China

ARTICLE INFO

Article history:
Received 12 August 2015
Accepted 9 December 2015

Keywords:
Polarization
Glints
Detection

ABSTRACT

For the purpose of investigating influence of waves on the performance of eliminating glints reflected off wavy sea surface by polarization filtering, we viewed glints twinkled in glitter path using a simultaneous multi-channel polarization camera. By analyzing the recorded data, it is found that the waving of water surface do not make unlimited influence on polarization elimination performance. Then a semi-quantitative analysis method is introduced. Combing with simulation results, it is concluded that the influence level of waves on polarization elimination performance is determined by observation geometry primarily and then limited by receiver's field of view. When observation geometry is approach to the Brewster condition closer, polarization filtering will has batter performance which is represented by more decrease of intensity of glints and lower influence level of waves on reducing intensity of glints.

1. Introduction

Glitter path is a bright and twinkling patch which can be seen on the ocean when the sea surface is ruffled by wind. In the glitter path, solar radiance reflected by the waving surface forms numberless glints which appear and disappear rapidly [1]. The sun glints formed by direct specular reflection of solar radiance has high brightness and can obscure the information that need to be acquired [2]. Coupled with the apparently random flash of glints, it makes a great challenge for tracing or directing target above water surface by airborne imaging equipment [3,4].

Utilizing polarization filtering to eliminate interventions caused by glints is one possible method to solve this problem [5]. According to the Fresnel law, water surface can be regarded as a polarizer [6]. So sun glints are partial linear polarized. And degree of linear polarization (DoLP) of glints may reach a high value (the maximum is 1) in part reflected direction. With the common situation that DoLP of man-made object with rough surface is usually low when object is illuminated by sunlight, polarization filtering can reduce more intensity of glints than target. So polarization filtering is potential to reduce the false alarms resulted from glints signally when water surface target detection is carried out.

Researches on polarization patterns of light reflected off water surface can provide foundation and guide for eliminating glints by polarization filtering. Gál et al. measured the reflection polarization pattern of the flat water surface under a clear sky firstly [7]. But under actual conditions, most of sea surfaces are not flat and calm but rough and waving [1,8]. Cox and Munk provided an analytical formula expressed by probability distribution of micro facets' slope to represent the relation between surface roughness and wind speed [9,10]. The changing of micro facets' slope causes the polarization properties of glints varying all the time [8]. Zhou et al. simulated the polarization patterns of skylight reflected off wave water surface in different conditions such as solar zenith angle, wind speed, wind direction and so on. Their investigation shows that the polarization pattern of skylight reflected off wave water can change slightly according to different wind conditions [11]. It means that polarization filtering also has potential to reduce the wave water reflection as flat water.

However, it is seldom investigated that how much influence resulting from waving of water surface will impact eliminating glints by polarization filtering in a receiver with certain field of view (FOV). In this paper, our experiments and simulations focused on analyzing the influence of waves and investigating the polarization elimination performance which includes the capability to reduce intensity of glints by polarization filtering under influence of waves and the influence level of waves on reducing intensity of glints. From experiments and simulations, it is found that the waving of water surface just has finite influence on polarization elimination performance. And the influence level of waves is determined by geometrical relation between sun and receiver primarily and then limited by receiver's FOV. In general, polarization

* Corresponding author. Tel.: +86 0431-86176958.
E-mail address: wangjianli@ciomp.ac.cn (J. Wang).

http://dx.doi.org/10.1016/j.ijleo.2015.12.057
0030-4026/

elimination performance on wave surface depends on the observation geometer. These conclusions acquired in this paper can provide valuable information for improving current airborne visible imaging equipment by utilizing polarization filtering to reduce the impact caused by glints.

2. Observation experiment

In order to analyze the influence on polarization elimination performance which resulted from waving of sea surface, observation experiments were carried out with help of a simultaneous polarization camera in Dalian (Liaoning province, China).

This simultaneous polarization camera (pixel size is 7.4 μm) is a division of focal plane polarimeter, which deposits pixilated micro-polarization filters array on the surface of CCD sensor. The micro-polarization filters array monolithically integrates 4 linear polarization filters (extinction ratio > 100:1 and transmission > 70% ranging from 400 nm to 900 nm) oriented at 0°, 45°, and 90° and 135° in a 2 × 2 array. The first three Stokes parameters (S_0,S_1,S_2) can be extracted by the intensity measurements from four photodiodes in the 2 × 2 array and are presented as following equation:

$$\begin{bmatrix} S_0 \\ S_1 \\ S_2 \end{bmatrix} = \begin{bmatrix} 1/2 & 1/2 & 1/2 & 1/2 \\ 1 & 0 & -1 & 0 \\ 0 & 1 & 0 & -1 \end{bmatrix} \begin{bmatrix} I_0 \\ I_{45} \\ I_{90} \\ I_{135} \end{bmatrix} \quad (1)$$

where I_0 is the intensity of the 0° filtered light wave, I_{45} is the intensity of the 45° filtered light wave, and so on. Then the DoLP and angle of linear polarization (AoLP) of incident light can be calculated by Eqs. (2) and (3) in real time,

$$\mathrm{DoLP} = \sqrt{\frac{{S_1}^2 + {S_2}^2}{S_0}} \quad (2)$$

$$\mathrm{AoLP} = \frac{1}{2} \cdot \arctan\left(\frac{S_2}{S_1}\right) \quad (3)$$

For purpose of observing glints with a long distance (about 1 km), the observation site located on a coastal cliff closed to sea.

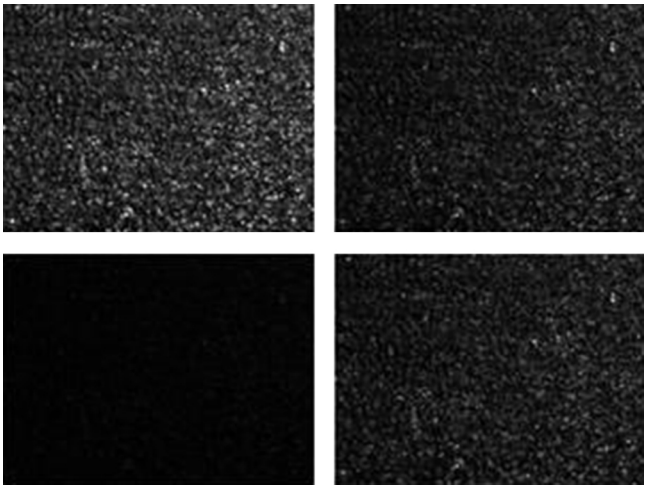

Fig. 1. Glints imaged in the four channels simultaneously. The left top, right top, left bottom and right bottom ones are imaged in 0°, 45°, 90° and 135° channels, respectively. In 90° channel, the reduction for intensity of glints has the best performance.

During our observation, solar elevation angle varied from 15.6° to 27.8°. And restricted by the coastal landform of observation site, camera's zenith angle can just change from 76° to 64°. We viewed along the centre line of glitter path to make glints twinkle in the whole camera's field of view (FOV). By keeping the included azimuth angle of sun and camera being 180°, the almost best polarization elimination performance could be achieved in the 90° channel of camera. So the polarization elimination ratio, which represents capability of reducing glins intensity by the ratio of glints intensity after and before polarization filtering, can be approximately calculated as I_{90}/S_0. The lower polarization elimination ratio (the optimal value is zero) is reached, the better polarization elimination performance can be achieved.

In order to analyze glints polarization properties and poalrization elimination ratio accurately, glints imaged in each channel should not be saturated. The images of glints recorded by the four

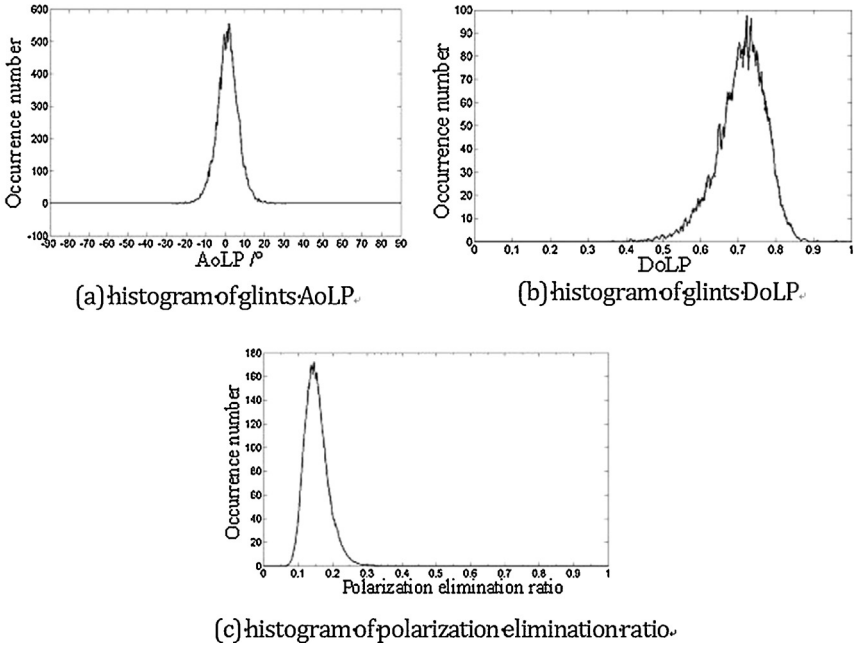

Fig. 2. Statistical conclusions for glints polarization properties and elimination ratio extracted from one single frame.

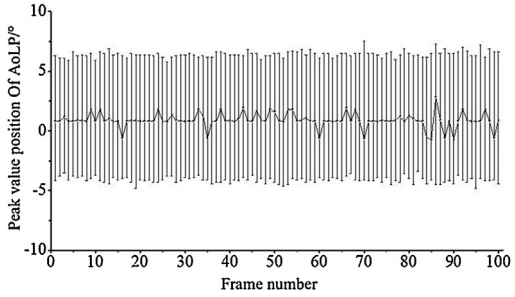

Fig. 3. Variation of peak value position and FWHM of AoLP extracted from the first continues 100 frames. The curve represents the peak value position of AoLP versus different frames. The error bars illuminates the FWHM of AoLP in corresponding frames.

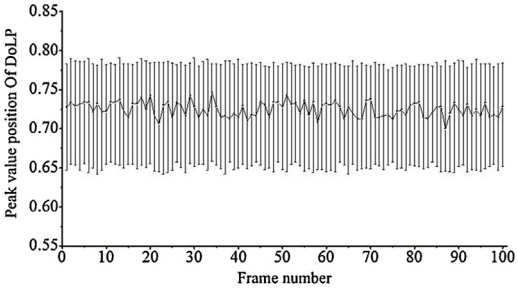

Fig. 4. Variation of peak value position and FWHM of DoLP extracted from the first continues 100 frames. The curve represents the peak value position of DoLP versus different frames. The error bars illuminates the FWHM of DoLP in corresponding frames.

channels are shown in Fig. 1. It is clear that glints imaged in 90° channel have obvious lower gray value than the others.

Glints changes so quickly that single snapshot is insufficient to understand influence from waving of sea surface. So we took videos (exposure time: 0.3 ms, frame frequency: 100 fps) contained 500 frames with a F15 lens of 50 mm focal length. Correspondingly, the camera's field of view is 6.8°.

After researching and analyzing the measurement data acquired in different time and observation conditions, the similar distribution and variance spread trend of glints polarization properties and polarization elimination performance can be found, except for the detail statistical values of those distributions and variance spreads.

To illuminate those distributions and variance spreads mentioned above, statistical analysis extracted from one video is shown below. During recording this video, wind direction was toward south and wind speed was between 7 m/s and 8 m/s. Solar elevation angle was 22.2° and camera's zenith angle was 74° with the included azimuth angle of sun and camera was 180°. The distance from the viewing area was about 1000 m.

Primal statistical analyses were carried out on one single frame and corresponding results are shown in Fig. 2. Fig. 2(a) shows the histogram distribution of glints AoLP which distributes in a certain range. The similar distribution trend can be found in Fig. 2(b) and (c), which represents the histogram distribution of glints DoLP and polarization elimination ratio. It can be find that, even influenced by waves, the polarization properties of glints just vary in a limited range. The same goes for the polarization elimination ratio.

To illuminate the variation among continue frames, peak value position and full width at half maximum (FWHM) of the histogram distribution mentioned above are introduced. The variance spreads of those two statistics values versus continue frames are shown in Figs. 3–5. The curve and error bars represent peak value position and FWHM, respectively. These spreads exhibit similar distribution trend that peak values fluctuate at certain value in a small range. In

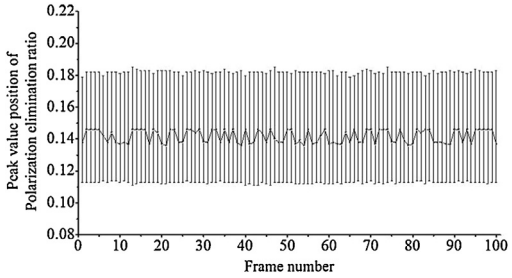

Fig. 5. Variation of peak value position and FWHM of polarization elimination ratio extracted from the first continues 100 frames. The curve represents the peak value position of polarization elimination ratio versus different frames. The error bars illuminates the FWHM of polarization elimination ratio in corresponding frames.

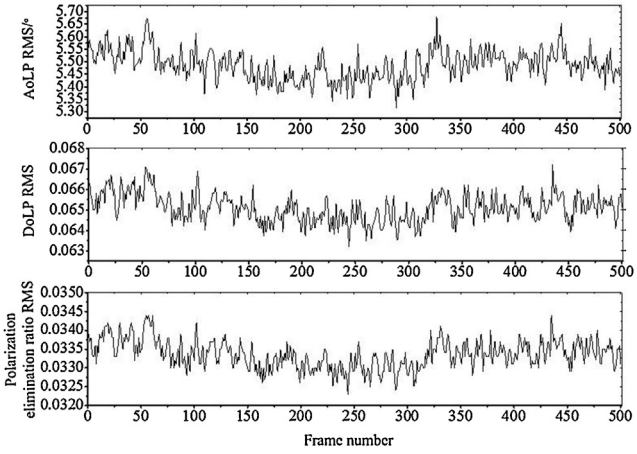

Fig. 6. RMS variance curves versus different frame. The top, middle and bottom curves represent RMS variances of AoLP, DoLP and polarization extinction ratio, respectively.

the same time, the positions and widths of FWHM only have little variance among different frames.

In addition, the root mean square (RMS) values of AoLP, DoLP and polarization elimination ratio over each frame, which can represent the corresponding average fluctuation level over the whole FOV, are analyzed. The RMS variances versus different frames, which are used to illuminate fluctuation versus continue frames, are shown in Fig. 6. These three curves fluctuate at certain value in a small range, too. So considering distribution trend in different FOV and variation among continue frames, the polarization elimination can stay in a limited and relatively stable state in the influence of waving of water surface.

Analyzing the rest video data recorded in our experiment, the detail statistical values of the distributions and variance spreads of glints polarization properties and polarization elimination ration only have small differences. So we don't list those values (part statistical values will be listed to compare with the simulation result in Section 4.1), distributions and variance spreads here. And it can be initially understood that the waving of water surface won't have a great and unlimited influence on the performance of polarization elimination in certain FOV.

Restricted by the landform of observation site, it was difficult to view sea surface with the real observation direction like practical target tracing or detection by airborne imaging equipment. So in the following sections, an analysis method is introduced and corresponding simulations are carried out to analyze the influence level of waves on polarization elimination performance further.

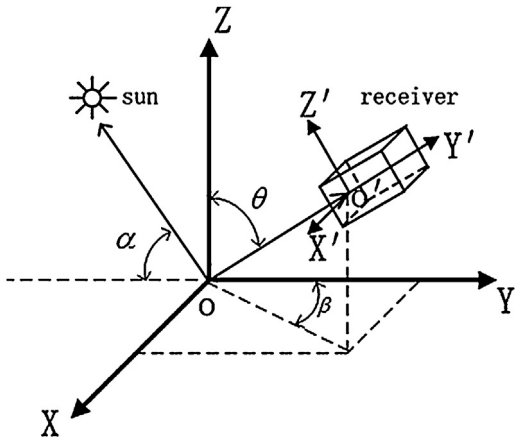

Fig. 7. Diagram of global observation coordinate system and receiver coordinate system.

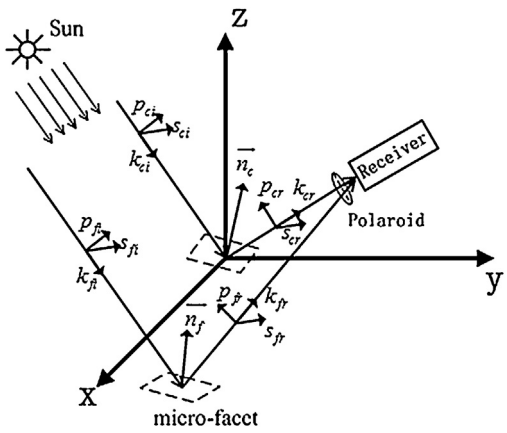

Fig. 8. Scheme of forming the polarization coordinate system in micro-facet model

3. Simulation methodology

3.1. Coordinate system

As shown in Fig. 7, a global observation coordinate system (right-handed system) is built according to the geometrical relation among sun, water surface and receiver's centre FOV. The *Z* axis is vertical to water surface and points upward. Correspondingly, the *Y* axis locates on the water surface and points toward the direction which makes the solar azimuth angle (related to *y* axis) equal to 180°. The XOY plane is parallel to horizontal water surface. So direction of sun can be specified by its elevation angle and azimuth in the form of (α, 180°).

In order to trace incident ray of receiver, another right-handed coordinate system represented as *X'Y'Z'* is formed. The coordinate system's origin is the center point of receiver's entrance pupil. The direction of *Y'* axis is same as receiver's. The *Z'* axis and *X'* axis point along the vertical and horizontal direction of receiver's sensor. Correspondingly, the transformation relation between the two coordinate system mentioned above can be expressed as Eq. (1).

$$\begin{bmatrix} x \\ y \\ z \end{bmatrix} = T_c \begin{bmatrix} x' \\ y' \\ z' \end{bmatrix} = \begin{bmatrix} \cos\ \beta & \sin\beta\sin\theta & -\sin\beta\sin\theta \\ -\sin\beta & \cos\beta\cos\theta & -\cos\ \beta\sin\theta \\ 0 & \sin\theta & \cos\theta \end{bmatrix} \begin{bmatrix} x' \\ y' \\ z' \end{bmatrix} \tag{4}$$

3.2. Polarization ray tracing

Related researches have shown that water wavy surface can be understood as a collection of micro-facets. In each micro-facet, water is considered to be specular and reflection process follows the Fresnel law [12–14]. Micro-facets of wave surface have different slopes and directions [10,11]. So according to geometrical optical principles, when the geometrical relation about incident solar direction, micro-facet slope and the direction of receiver's FOV meets the law of reflection, solar radiance reflected by micro-facets will enter receiver and form sun glitter [15].

To analysis the polarization properties of the rays reflected by micro-facets, each ray's polarization coordinate system is formed as following. This coordinate system represented by ***psk*** is a right-handed system with the ***k*** axis pointing toward the ray's propagation direction, the ***s*** and ***p*** axis pointing vertical and parallel to the incident plane, respectively. Taking two rays entering different FOV of receiver which are reflected by the micro-facets and represented by normal vectors $\vec{n_c}$ and $\vec{n_f}$ as example, the construction of polarization coordinates is illustrated in Fig. 8. Correspondingly, coordinate $p_{ci}s_{ci}k_{ci}/p_{cr}s_{cr}k_{cr}$ and $p_{fi}s_{fi}k_{fi}/p_{fr}s_{fr}k_{fr}$ are the polarization coordinates for incident and reflected ray of micro-facet $\vec{n_c}$ and $\vec{n_f}$, respectively.

Using unit vector to express each axis' direction in polarization coordinate system, such as vector $\vec{k_{ci}}$ and $\vec{k_{ci}}$ denoting the direction of axis k_{ci} and k_{ci}, the relation of polarization coordinates between incident and reflected ray can be expressed as following equation:

$$\begin{cases} \vec{n_c} = \vec{k_{ci}} \times \vec{k_{cr}},\ \vec{s_{ci}}\vec{s_{cr}},\ \vec{p_{ci}} = \vec{s_{ci}} \times \vec{k_{ci}},\ \vec{p_{cr}} = \vec{s_{cr}} \times \vec{k_{cr}} \\ \vec{n_f} = \vec{k_{fi}} \times \vec{k_{fr}},\ \vec{s_{fi}}\vec{s_{fr}},\ \vec{p_{ci}} = \vec{s_{ci}} \times \vec{k_{ci}},\ \vec{p_{cr}} = \vec{s_{cr}} \times \vec{k_{cr}} \end{cases} \tag{5}$$

In each ray's polarization coordinate system, the polarization analysis of light can be accomplished by coherence matrix and corresponding matrix operation. Then combining with global observation coordinate and receiver coordinate formed above, the polarization ray tracing of rays entering receiver can be achieved.

3.3. Analysis method

When searching or tracing target above sea surface by airborne image equipment, fast movement state of the aerial vehicle always makes wind direction relative to receiver changing all the time. In addition, with the observation geometer changing, the polarization properties of the glints which may deteriorate receiver's sensor vary accordingly. So it is a great challenge to form the actual instantaneous distribution of wave surface to analysis the corresponding polarization elimination performance. For analyzing the performance of polarization elimination under influence of wave in different observation situations, a semi-quantitative analysis method is introduced below. We skip the actual instantaneous distribution of wave surface and assume that each FOV of receiver shall be affected by glints uniformly. In other words, it is assumed that, in any viewing moment, the distribution of wave surface is in the state which will make the entire receiver's sensor overflowing with glints.

4. Simulation and discussion

Using the methods mentioned above, with ignoring the influence from skylight and assuming that incident sunlight is just consisted of parallel rays. Corresponding simulation results and related analysis are discussed as follow.

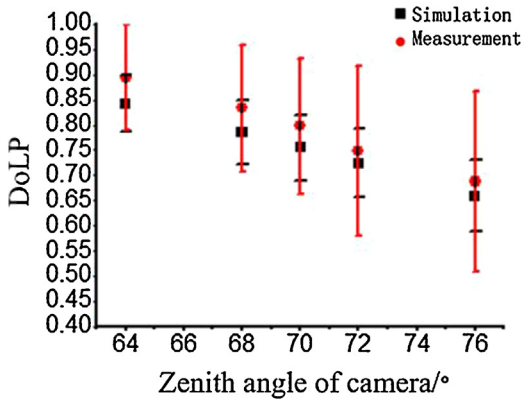

Fig. 9. Comparisons of mean DoLP between the measurement data and simulation result.

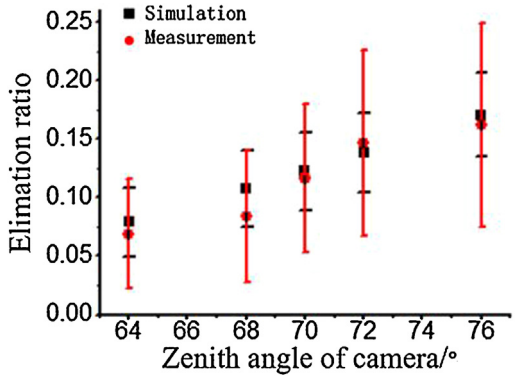

Fig. 10. Comparisons of mean elimination ratio between the measurement data and simulation result.

4.1. Comparison of measurement and simulation

In simulation, the Polaroid used to elimination glints is located in front of receiver's lens. Refractive index of seawater is chosen as 1.34. The receiver's FOV is set to 6.8° which matches to the simultaneous polarization camera used in experiment.

The Polaroid can only choose one rotation angle which cannot reach the optimal mean for different FOV. By analyzing (detailed description is shown in Section 4.2), making the mean polarization elimination ratio minimum is chosen as standard to select Polaroid rotation angle. In order to test the availability of this simulation method, the comparison between a set of measurement data recorded in experiments and simulation results in the same observation geometer (solar elevation angle is 26.3° and camera's zenith angle varies for 76° to 64°) are shown in Figs. 9 and 10. In Fig. 9, the red dots represent mean DoLP values which are calculated over the whole camera's FOV and then taken the mean from continus 500 frames in one video data. The red error bars represent the mean FWHM of DoLP over continus 500 frames. The balck squares and error bars represent corresponding simulation results.

It can be found that, the simulation results and measurement data have similar values and variance trend versus different observation direction, except that the mean FWHM values extracted from measurement data are bigger than simulation's. So this simulation method is reliable to analyze the polarization elimination performance when glints may twinkle the entire receiver FOV. The divergence between measurement and simulation mainly results from following causes:

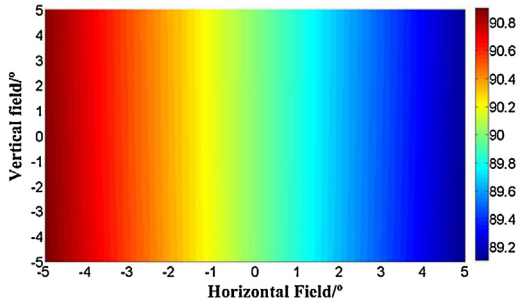

Fig. 11. The optimal rotation angle of Polaroid distribution over receiver's FOV.

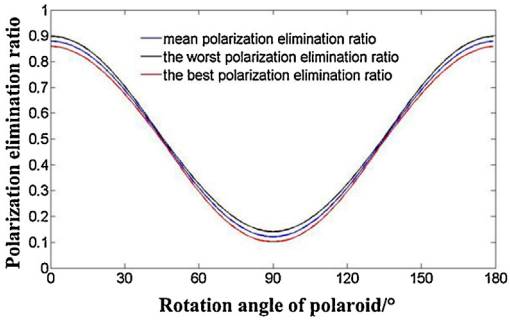

Fig. 12. Polarization elimination ratio curves versus different Polaroid's rotation angles

(1) The practical distribution of wavy sea surface is varying all the time and different from assumption in simulation.
(2) Influence from skylight is ignored in simulation.

In summary, this simulation method can be considered to be available when glints twinkle in the whole FOV of camera. It can be used as a semi-quantitative simulation method to analyze the influence level of waves and the polarization elimination performance under influence of waves.

4.2. Simulations of polarization elimination performance and analysis

In simulations, solar elevation angle and receiver's zenith angle are set to 10° and 0° with receiver's azimuth equal to 0°. The Polaroid used to elimination glints is located in front of receiver's lens. Refractive index of seawater is 1.34. Receiver's FOV is set to $10° \times 10°$ with sampling interval of 0.01°.

The optimal rotation angle (anticlockwise to *X*' axis in receiver coordinate system) of Polaroid for reducing intensity of glints twinkled in corresponding FOV is shown in Fig. 11. The variance range over the entire FOV is small. So it is beneficial to use polarization filtering to reduce the intensity of glints.

The Polaroid can only choose one rotation angle which won't meet the optimal orientation in different FOV. So we simulated the process of rotating Polaroid and analyzed corresponding variance of polarization elimination ratio. The curve of mean, the best and the worst polarization extinction ratio versus different Polaroid's rotation angles are shown in Fig. 12. It can be seen that the three curves show similar variance trend. When Polaroid rotates to 90°, the best polarization elimination ratio is achieved. So making the mean polarization elimination ratio minimum is chosen as a standard to select Polaroid rotation angle in following simulations.

The polarization elimination ratio distribution over the entire FOV is shown in Fig. 13, in which mean polarization elimination ratio achieves the best level with Polaroid rotating to 90°.

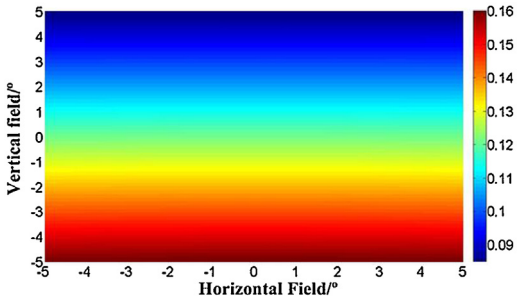

Fig. 13. Polarization elimination ratio distribution over receiver's FOV.

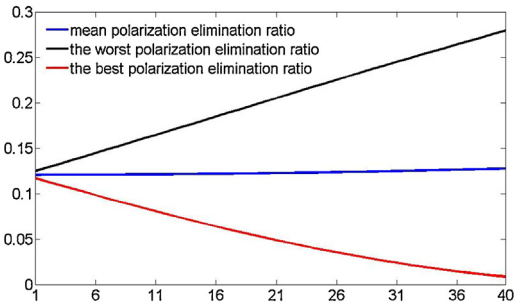

Fig. 14. Variance of polarization elimination ratio with increasing of receiver's FOV.

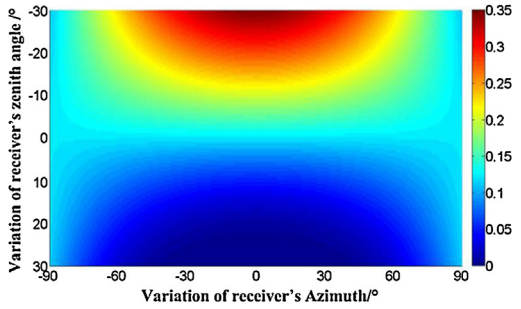

Fig. 15. The best mean polarization elimination ratio distribution with changing of receiver's azimuth and zenith angle.

Based on the simulation conditions mentioned above, the polarization elimination ratio in the condition of different FOV is simulated with changing receiver's FOV from 1° to 40°. The curve of mean, the best and the worst polarization elimination ratio versus increasing receiver's FOV are shown in Fig. 14. With the receiver's FOV increasing, mean polarization elimination ratio changes little and the diversity between the best and the worst polarization elimination ratio becomes bigger. It indicates that increasing of receiver's FOV will raise the difficulty of deducing glints intensity by one Polaroid.

Then receiver's zenith angle and azimuth are changed to analyze polarization elimination performance in different viewing direction of receiver. The best mean polarization elimination ratio distribution versus variation of receiver's azimuth and zenith angle is shown in Fig. 15. The positive direction of receiver's zenith variance matches the increase of included angle between sun and receiver. It can be considered that, when variance of receiver's zenith angle is positive, receiver is in the "against-light" state. In this moment, receiver will be compacted by glints more easily and seriously than "front-light" state which is corresponding to negative variance of receiver's zenith angle. As shown in Fig. 15, polarization filtering can reduce the intensity of glints effectively when receiver is in "against-light" state even under influence of waves. But little polarization elimination effect is acquired in "front-light" state.

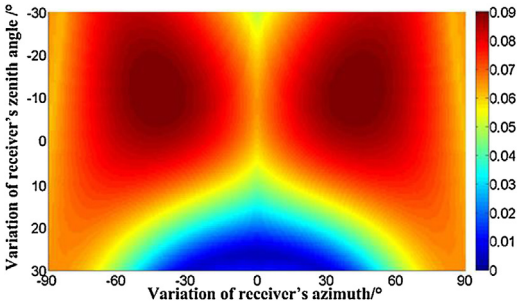

Fig. 16. PV value distribution of polarization elimination ratio with changing of receiver's azimuth and zenith angle.

Then peak-to-vale (PV) value of polarization elimination ratio is introduced to represents the max diversity of polarization elimination ratio over the entire FOV. Distribution of the PV value versus variation of receiver's azimuth and zenith angle is shown in Fig. 16. The PV value, which can be used to evaluate the influence level of waves on polarization elimination qualitatively, changes with variance of receiver's observation direction and has similar variance trend to polarization elimination ratio. It indicates that, in the same conditions of wind and waves, the waving of water surface makes different levels of influence on polarization elimination in different viewing direction. This is because that polarization properties of glints imaged in receiver's sensor are determined by the incident angle and direction of incident plane of corresponding incident sunlight and limited by receiver's FOV. The variance range of PV value maintains in a low level. This can be understood that the waving of water surface just has finite influence on polarization elimination.

4.3. Discussion

From the simulation results acquired above, it can be found that waves will make polarization properties of glints entering receiver FOV differently. This increases the difficulty of reducing glints intensity by polarization filtering. But limited by receiver FOV and geometrical relation between sun and receiver, polarization elimination ratio over the entire receiver FOV won't distribute disorderly and unlimitedly in the influence of waves. It is beneficial to reduce the impact of glints effectively even under influence of waves. The similar distribution trend versus viewing direction of polarization elimination ratio and its PV value over entire FOV indicates that polarization elimination performance will be determined by solar elevation angle and viewing direction of receiver. Here we introduce Brewster condition to represent that glints entering receiver FOV are reflected off water surface with the Brewster angle. The polarization elimination performance will become better when the "Brewster condition" is approached closer. As well as the simulation result showed in Figs. 15 and 16, polarization elimination performances better in the "against-light" state. Because in this situation, the reflection angle of glints are closer to the Brewster angle.

In most duties of detecting or tracing target above water surface by airborne imaging equipment, solar elevation angle will be kept in a low level. It is advisable to reduce the impact of glints when imaging equipment is in "against-light" state which may make glints twinkle in receiver's sensor more possibility. Further, combining with rotating Polaroid to the optimal orientation under real time control, polarization filtering predicts to reduce the impact of glints effectively. What's more, this real time controlled polarization filtering can be relatively easy to achieve by improving current visible imaging equipment. So it is potential to promote performance of

current airborne visible imaging equipments under impacting of glints.

5. Conclusion

We observed glints reflected off wave water on glitter path using a simultaneous polarization camera and analyzed the performance of polarization elimination under influence of waves. Then a semi-quantitative analysis method, which assumes glints will twinkle in any FOV of receiver, is used to analyze the influence level of waves and simulated polarization elimination performance under influence of waves in different observation conditions such as receiver FOV, solar elevation and viewing direction. Combining with experiments and simulations, it can be found that waves will make polarization properties of glints entering receiver FOV differently. But limit by receiver's FOV and geometrical relation between sun and receiver, the polarization elimination ratio won't distribute disorderly over receiver FOV under influence of waves. And the waving of water surface won't make polarization elimination performance vary unlimitedly versus continue imaging frames.

From simulation we also find that, in the same conditions of wind and waves, the influence level of waves on polarization elimination varies with the changing of viewing direction. In general, the influence level of waves is determined by geometrical relation between sun and receiver primarily and then limited by receiver's FOV. It can be concluded that polarization elimination performance under influence of waves depends on geometrical relation between sun and receiver chiefly. The closer the "Brewster condition" is approached, the better polarization elimination performance which represented by stronger decrease of glints intensity and lower influence level of waves on polarization elimination is achieved.

The analysis method used in this paper is semi-quantitative with some approximates and needed to be improved by further study. But the conclusions acquired by this method can provide prediction and preparation for polarization elimination in the field of water surface target trace of detection by airborne visible equipment which will be carried out in following study.

Acknowledgements

This work was supported by the 863 Program (2014AAXXXX072D). The authors appreciate all of the help and suggestions from our schoolmates and colleagues during this research. We are grateful to reviewers for their valuable comments.

References

[1] David K. Lynch, David S.P. Dearborn, James A. Lock, Glitter and glints on water, Appl. Opt. 50 (2011) F39–F49.
[2] S. Kay, J.D. Hedley, S. Lavender, Sun glint correction of high and low spatial resolution images of aquatic scenes: a review of methods for visible and near-infrared wavelengths, Remote Sens. 1 (69) (2009) 7–730.
[3] S.P. Garaba, O. Zielinski, Methods in reducing surface reflected glint for ship-borne above-water remote sensing, J. Eur. Opt. Soc. Rap. Public 8 (2013) 13058.
[4] Alessandro Rossi, Aldo Riccobono, Stefano Landini, Sun-glint false alarm mitigation in a maritime scenario, Proc. SPIE 9250 (2014) 92500X.
[5] Alex Cunningham, Peter Wood, David McKee, Brewster-angle measurements of sea-surface reflectance using a highresolution spectroradiometer, J. Opt. A: Pure Appl. Opt. 4 (2002) S29–S33.
[6] Gábor Horváth, Dezsö Varjú, Polarization pattern off reshwater habitats recorded by video polarimetry in red, green and blus spectral ranges and its relevance for water detection by aquatic insects, J. Exp. Biol. 200 (1997) 1155–1163.
[7] József Gál, Gábor Horváth, Viktor Benno Meyer-Rochow, Measurement of the reflection polarization pattern of the flat watersurface under a clear sky at sunset, Remote Sens. Environ. 76 (2001) 103–111.
[8] M. Ottaviani, C. Merck, S. Long, J. Koskulics, K. Stamnes, W. Su, W. Wiscombe, Time-resolved polarimetry over water waves:relating glints and surface statistics, Appl. Opt. 47 (2008) 1638–1648.
[9] C. Cox, W. Munk, Measurement of the roughness of the sea surface from photographs of the sun's glitter, J. Opt. Soc. Am. 44 (1954) 838–850.
[10] C. Cox, W.H. Munk, Slopes of the sea surface deduced from photographs of sun glitter, Scripps Inst. Oceanogr. Bull. 6 (1956) 401–487.
[11] Guanhua Zhou, Wujian Xu, Chunyue Niu, Huijie Zhao, The polarization patterns of skylight reflected off wave water surface, Opt. Exp. 21 (2013) 32549–32565.
[12] John A. Guinn Jr., Gilbert N. Plass, George W. Kattawar, Sunlight glitter on a wind-ruffled sea: further studies, Appl. Opt. 18 (1979) 842–849.
[13] Egbert Tse, John McGill, Coherent Whitecap and Glitter simulation model, Proc. SPIE 1302 (1990) 505–519.
[14] C.R. Zeisse, C.P. McGrath, K.M. Littfin, Infrared radiance of the wind-ruffled sea, J. Opt. Soc. Am. A 16 (1999) 1439–1452.
[15] José Luis Poom-Medina, Josué Álvarez-Borrego, Beatriz Martín-Atienza, Ángel Coronel-Beltrán, Theoretical statistical relationships between the intensities of an image of the sea surface and its slopes: a result comparison of RECT and Gaussian glitter functions, Opt. Eng. 53 (2014) 043103.